


## Research Article

# Model-Based Predictive Detector of a Fire inside the Road Tunnel for Intelligent Vehicles

**Marián Hruboš** <sup>1</sup>, **Dušan Nemec**,<sup>1</sup> **Emília Bubeníková**,<sup>1</sup> **Peter Holečko**,<sup>1</sup> **Juraj Spalek**,<sup>1</sup> **Michal Mihálik**,<sup>1</sup> **Marek Bujňák**,<sup>1</sup> **Ján Anđel**,<sup>1</sup> and **Tomáš Tichý**<sup>2</sup>

<sup>1</sup>Department of Control and Information Systems, Faculty of Electrical Engineering and Information Technology, University of Žilina, Žilina, Slovakia

<sup>2</sup>Department of Transport Telematics, Faculty of Transportation Sciences, Czech Technical University, Prague, Czech Republic

Correspondence should be addressed to Marián Hruboš; [marian.hrubos@feit.uniza.sk](mailto:marian.hrubos@feit.uniza.sk)

Received 8 October 2020; Revised 26 January 2021; Accepted 2 February 2021; Published 12 February 2021

Academic Editor: Petr Dolezel

Copyright © 2021 Marián Hruboš et al. This is an open access article distributed under the Creative Commons Attribution License, which permits unrestricted use, distribution, and reproduction in any medium, provided the original work is properly cited.

The paper proposes a method for detection of a fire inside the road tunnel without direct view on the fire, using on-board vehicle technologies. The system is based on comparing the measured development of temperature and smoke with model scenarios precomputed for a given road tunnel. The fire scenarios are computed by HW/SW tool TuSim regarding the parameters of the real road tunnel and then the results are presented to the vehicles via car-to-infrastructure communication link. The proper detection of the fire allows early evacuation of the vehicle passengers, which will significantly increase chance of their survival. The computed scenarios also provide supporting information for the rescue teams.

## 1. Introduction

Safety of transported persons and material is an integral part of today's transport. From the viewpoint of risk and subsequent damage, the worst place is the road tunnel. In case of accident, several dangerous situations occur in the tunnel. One of the most dangerous accidents at all is the fire inside the tunnel. Even when the fire is detected by sensors and cameras installed in the tunnel tube, statistics says that not all passengers in the threatened zone will evacuate from the vehicles in time. We believe that this drawback can be suppressed when not only the operators of the tunnel but also the vehicles themselves are sensing and detecting the indicators of the fire-rising temperature and opacity.

Subsequent recovery after the accident is also challenging and can expose other persons to danger. Therefore, we propose a simulation model that is able to estimate situation in the tunnel during an accident event. Furthermore, such information can be utilized by rescue teams.

The paper deals with an effect of the technological equipment on safety of humans and property in the tunnel.

To reach a tolerable level of safety, the heterogeneous complementary systems must be installed in the tunnel. The numerical expression of the risk is problematic. Therefore, simulation is one of few possibilities of how to safely compare various variants and test the system limits, so-called worst cases, as an alternative to the prescriptive risk analyses. This paper is focused on the simulation of critical scenarios itself, on the creation of trustworthy models and their subsequent verification and validation.

Nowadays, the tunnel simulators may be classified to the following groups:

- (1) Simulators used to train tunnel operators, dealing mainly with virtual reality or tunnel visualization [1].
- (2) Drive simulators used to train drivers driving through the tunnel; they make it possible to monitor and analyse drivers' behaviours, technical parameters of their drives, minds, subjective feelings, etc. [2].
- (3) Specialized simulation tools such as IDA RTV software [3].

- (4) Simulators based on the PLC (programmable logic controller) that are mostly used to verify control of tunnel technologies under various modes before putting the control system into operation [4, 5]. These simulators may utilize additional specialized tools for simulation of the tunnel technology and physics; an architecture of such a simulator is depicted in Figure 1.

Fire, in general, can be detected by the following way:

- (1) SOS button
- (2) Video detection
- (3) Smoke sensors
- (4) FibroLaser line detector

In principle, video detection can detect a fire in several ways, by detecting a car/vehicle stop, fire, or smoke in the monitored zone. In time, this method is the fastest method; on the other hand, false alarms can occur from the smoke in tunnel through the passage of truck or light reflection. In this case, in Slovakia the tunnel is usually closed only after approval by the operator. The detection of stopped vehicle is almost immediately. There are two types of smoke sensors: opacity sensors of specialized smoke sensors. Opacity sensors must be installed closed to portal, branching at maximum distance of 1000 meters along tunnel. According the manufacture's materials SIGRIST, the opacity sensors have a measuring range of 0–100 km; accuracy in the range 0–15 km must be  $\pm 2$  km. These sensors can be also used for fire detection; they are usually installed on the wall of the tunnel. Smoke sensors must be installed at the maximum distance of 150 meters along tunnel. The measure range of these smoke sensors is 0–15 km and accuracy is 0, 2 km; they are usually installed on the tunnel ceiling.

Typical values in measuring opacity:

- (1) Normal traffic <5 km
- (2) Heavy traffic ~5 km
- (3) Traffic jam ~7 km
- (4) Tunnel close 12 km
- (5) Fire >15 km

FibroLaser detects an increased heat in fire in the tunnel. It is built up of optical cables and control unit that emits a laser beam into the cable and analyses its reflection. There is a Raman effect, when the reflected laser beam is divided into Stokes and AntiStokes signal and temperature change in optic cable is evaluated based on the difference in the intensity of these signals. It is possible to implement FibroLaser into simulation programs according the data of the manufacturer Siemens. There are three rules for how to detect the increase in temperature:

- (1) Overrun defined maximum value
- (2) Overrun the maximum difference from the average temperature zone
- (3) Overrun the maximum increase of temperature in define time

## 2. Tunnel Simulator TuSim

The tunnel simulator (TuSim), developed by the authors of the article, is based on the programmable logic controller (PLC). The TuSim is a complex HW/SW solution based on the industrial personal computer (PC), Bernecker and Rainer (BR) Automation PC acting as a PLC. The TuSim is shown in Figure 2 and consists of (top-down view) the Masterview liquid-crystal-display (LCD) switch of the visualization server, BR Automation PC (in the left bottom), and the backup UPS unit (in the right bottom). The uninterruptible power supply (UPS) unit ensures simulation of the continuous operation.

In the BR Automation PC, the PLC of Siemens S7-400 type is simulated including the technological components as well. The TuSim simulator makes it possible to simulate three types of the tunnel, 1000 m long each:

- (1) Urban tunnel (MST)
- (2) Highway one-tube tunnel (D1T)
- (3) Highway two-tube tunnel (D2T)

Visualization of technological equipment is ensured through the human-machine interface/supervisory control and data acquisition (HMI/SCADA) displays. The whole system has an open software concept for future extensions from the level of software in the PLC up to the design of graphical screens.

The simulator is not connected to the data flow of a real tunnel. The HMI server takes care of data collection, archiving, and distribution from PLC clients. Selection of data to be archived in the database at the server is configured by the Database Logger [6], and then data may be shown in all clients. In addition to data display, the clients also make it possible to perform control interventions in displays individually for each technological sub-system. To display and change the screens, the tools CimViewer and CimEdit [7] from the HMI/SCADA CIMPLICITY software are being used.

For the reason of model verification, the PLC may be interconnected to other tools in the following ways:

- (1) Extensible markup language (XML) interface provided by the ELTODO company
- (2) Libnodave dynamic-link library (DLL library) [8]
- (3) MATLAB/SIMULINK [9]
- (4) IDA road tunnel ventilation (RTV) [3]

## 3. Simulation Models

In the first version, the TuSim was a drive simulator helping service operators to become familiar with the control system of the tunnel and to simulate emergency events manually via so-called reflexes. Since no mathematical-physical models, needed to simulate functionality of the many tunnel systems, were built-in, they had to be integrated additionally. Figure 3 shows models important for basic functionality and interactions between them. The models in blue fields are implemented directly on the PLC level, others on the HMI/SCADA level.

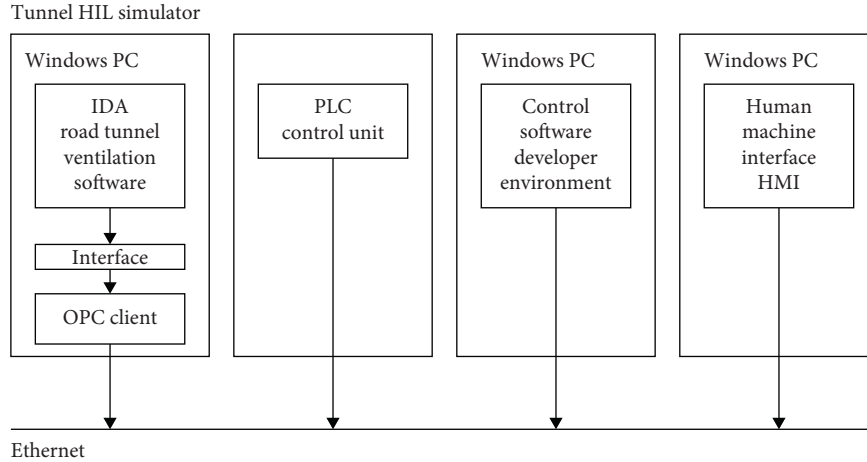


FIGURE 1: Architecture of the PLC-based Hardware-in-the-Loop (HIL) tunnel simulator [5].



FIGURE 2: TuSim.

**3.1. Traffic Flow Model.** As it is apparent from Figure 3, the model of air flow processes the piston effect resulting from the movement of vehicles inside the tunnel as one of its inputs. Under the one-way traffic, vehicles put the air to motion. The more significant the contribution of that, the higher the volume of vehicle intensity. Products of combustion in the tunnel are also an important input to control air technology. It is also important to know composition of traffic flow, since trucks and buses have much higher impact on emissions in the tunnel environment. More information about the traffic model of the TuSim is in [10–12].

**3.2. Tunnel's Tube Model.** The tunnel tube may be modelled by multiple ways. One of them is based on analysis of the relationship between its inputs and outputs. This approach has been used in [13]. To describe a linear part of the model, we used the state model. The non-linear part of the model includes saturation and transport delay. The model of the tunnel tube is expected to enable changing of carbon monoxide CO and nitrous oxides NO<sub>x</sub> sensors positions. That will make it possible to monitor variances in ventilation control. Concentration of emissions in time and space may be calculated using the equation for the longitudinal ventilation [14]:

$$\frac{\partial C}{\partial t} + \frac{\partial(vC)}{\partial x} = e_c, \quad (1)$$

where  $t$  is time of simulation (s) and  $x$  is distance (m).

If the measured and calculated velocity of the air flow in the tunnel is available, we can immediately use solution of the equation from [14], for example, for the values of CO in a steady state:

$$C(x) = \frac{e_c}{v} + C(0), \quad (2)$$

$$e_c = \frac{NE}{3.6v_v A'},$$

where

- (1)  $C(0)$  is the concentration of CO at the input portal of the tunnel ( $\mu\text{g}/\text{m}^3$ )
- (2)  $v$  is the velocity of the air flow in the tunnel (m/s)
- (3)  $v_v$  is the average velocity of the vehicle movement (km/h)
- (4)  $N$  is the traffic volume (veh/h)
- (5)  $E$  is the COemissions of the vehicle (g/h.veh)
- (6)  $A$  is the tunnel cross section ( $\text{m}^2$ ), and  $A'$  is a derivation of  $A$

In our model, the values of emissions for all velocities and gradients are stored in the table. Outputs of the model of

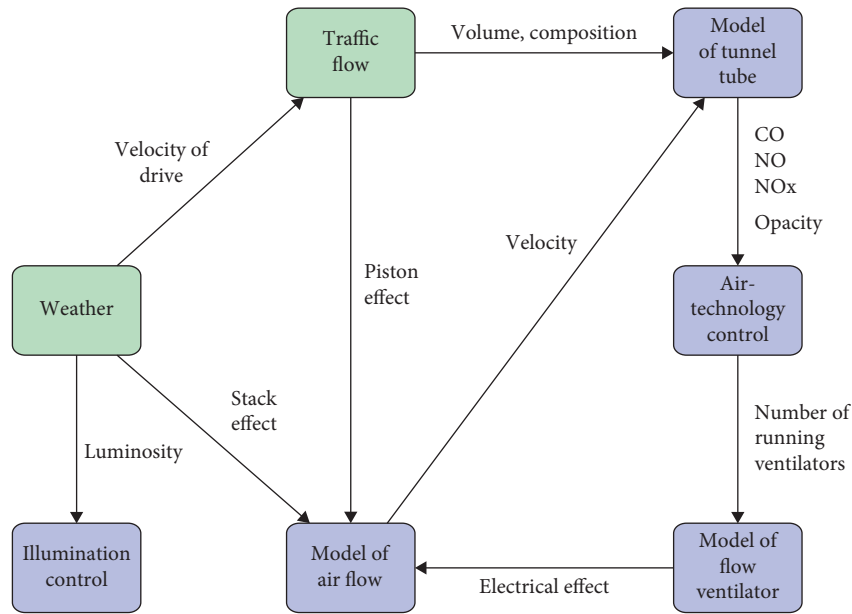


FIGURE 3: Interactions among modules of the extended simulation model TuSim.

the longitudinal ventilation for one-way traffic will create a linear function, with growing concentration of CO emissions towards the output portal of the tunnel. In [15], there are a discrete microscopic traffic model and emissions modelled for each section occupied by a vehicle according to the tables of emissions [16]. The advantage is that emissions from vehicles do not depend on shape of the tunnel; thus, the model may be used universally. Figure 4 shows comparison of our traffic model extended for the model of the tunnel tube with the model of steady state conditions.

After velocity of the air flow becomes stabilized, the values of CO emissions in the microscopic model are close to the values of emission models of the macroscopic traffic model along the whole length of the tunnel. For the needs of the traffic model, we have adopted the PIARC tables [16] for discrete velocities used in the traffic model – 0 (km/h), 30 (km/h), 50 (km/h), maximum velocity in the tunnel 80 (km/h), maximum gradient 4%.

**3.3. Air Flow Model.** Simulation of the air flow in the tunnel is a complex problem demanding numeric solution of Navier–Stokes non-linear differential equations. Their solution is too time demanding to be used in the real-time in the PLC. As an alternative, one might use Bernoulli equation for one-dimensional liquid flow while we consider that the air is as an incompressible fluid:

$$\frac{1}{2}\rho v^2 + \rho gh + p = \text{const. for } p \sim \text{const.} \quad (3)$$

where

- (1)  $\rho$  is the air density ( $\text{kg m}^{-3}$ )
- (2)  $v$  is the air velocity (m/s)
- (3)  $p$  is the pressure ( $\text{Nm}^{-2}$ )

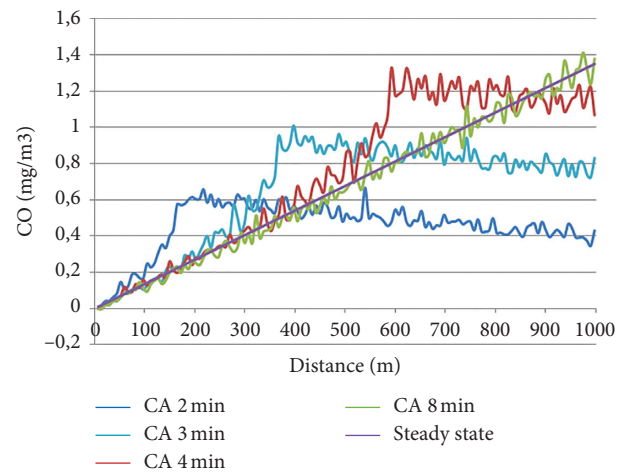


FIGURE 4: Comparison of models of CO emissions.

(4)  $h$  is the height difference between the ends of the tunnel (m)

(5)  $g$  is the gravitational acceleration ( $\text{ms}^{-2}$ )

This formula is valid only in the case of an ideal liquid; in the case of real liquid, the equation must be extended for a member representing friction losses. Velocity of the flow in the tunnel is influenced by many factors: difference in temperatures between the tunnel and outside environment, gradient of the tunnel, piston effect, effect of fans, friction, change of the cross section, weather conditions at the portal, etc. In our case, the majority of Slovak tunnels have non-rugged profiles; i.e., their cross section is the same, and so only one equation must be solved. Otherwise, a system of equations should be solved for each section of the tunnel in the case of the profile change, branching-off inside the tunnel, when the ventilation shaft is used (Branisko tunnel)

or combined ventilation systems (Višňové tunnel being under construction) [17].

In order to compare the methods, we have created a model similar to the Bôrik tunnel in the IDA RTV [6], with circumference  $P = 29.22$  m and cross section area  $A = 57.26$  m<sup>2</sup>. To calculate the air flow, we used the substitutionary circular cross section of the tube whose hydraulic diameter  $D$  can be calculated [18]:

$$D = \frac{4A}{P} = \frac{4(57.26)}{29.22} = 7.83846 \text{ (m)}. \quad (4)$$

Flow fans put air to motion; pressure change depends on a number of fans, efficiency, and fan area. References [19, 20] give multiple versions of the equation for both mobile fans and ceiling flow fans:

$$\Delta P_{\text{FAN}} = \frac{\eta I_{\text{FAN}}}{A} \left( 1 - \frac{v}{v_{\text{FAN}}} \right), \quad (5)$$

where

- (1)  $A$  is the area of tunnel cross section (m<sup>2</sup>)
- (2)  $\eta$  is the efficiency of the fan (%)
- (3)  $I_{\text{FAN}}$  is the pushing force of the fan (N)
- (4)  $v$  is the velocity of the air flow (m/s)
- (5)  $v_{\text{FAN}}$  is the velocity of the fan air (m/s)

For one-way traffic, the moving vehicles move air in the tunnel on, creating so-called piston effect. The higher the velocity and traffic volume are, the higher this effect is. Due to emergency situations in the tunnel, we are also interested in the situation with stopped vehicles when their velocity is lower than velocity of air flow in the tunnel. Since air flow decelerates, we used the equation with the absolute value of velocity [21]:

$$\Delta P_{\text{PISTON}} = \frac{\sum_{i=0}^4 N_i C_i A_i}{2A} \rho |v_v - v| (v_v - v), \quad (6)$$

where

- (1)  $A$  is the area of the tunnel cross section (m<sup>2</sup>)
- (2)  $\rho$  is the air density (kg/m<sup>3</sup>)
- (3)  $v$  is the velocity of air flow (m/s)
- (4)  $v_v$  is the velocity of vehicles (m/s)
- (5)  $N_i$  is the number of vehicles
- (6)  $A_i$  is the front area of the vehicle (m<sup>2</sup>)
- (7)  $C_i$  is the friction coefficient

Under fire conditions, temperature in the tunnel will increase which will cause temperature difference between internal temperature and temperature of surrounding environment. The fire represents barrier to air flow. The local loss of pressure caused by the fire depends on temperature power, shape of the lateral cross section of the tunnel, and other factors. The most accurate way of determining temperature in the tunnel is using the CFD simulation or evaluation of real fire experiments. The average temperature in the whole fire section may simplistically be calculated [17]:

$$T_m = T_0 + (T_{\text{fire}} - T_0) \exp\left(\frac{-\alpha P}{v \rho A c_p} x\right), \quad (7)$$

where

- (1)  $\rho$  is the air density (kg/m<sup>3</sup>)
- (2)  $A$  is the area of the tunnel cross section (m<sup>2</sup>)
- (3)  $T_0$  is the temperature in front of the place of fire (K)
- (4)  $T_{\text{fire}}$  is the temperature at the place of fire (K)
- (5)  $\alpha$  is the coefficient of the heat transfer (W/m<sup>2</sup>K)
- (6)  $P$  is the circumference of the tunnel (m)
- (7)  $c_p$  is the specific heat capacity of the air (kJ/(kgK))
- (8)  $x$  is the distance from the place of fire (m)

The final differential equation of the air flow velocity was obtained as sum of all mentioned pressure differences and also others described in [22]:

$$\frac{dv}{dt} = \frac{\sum \Delta P}{\rho L}, \quad (8)$$

where

- (1)  $\Delta P$  is the all elements mentioned above (Pa)
- (2)  $\rho$  is the air density (kg/m<sup>3</sup>)
- (3)  $L$  is the length of the tunnel (m)

Furthermore, other members of the equation, such as the temperature differences and the influence of the wind, can be considered.

**3.4. Fire Model.** The course of the fire may be simulated in various tools. For the reason of calculation time, the three-dimensional simulation by the fire dynamics simulator (FDS) was excluded. There may be two-dimensional simulation using CFAST [23] taken into account which is primarily designed for simulation of the fire in buildings. CFAST was extended for simulation of air flow in long corridors. In [24], the tunnel consisted of several interconnected corridors for the zone model; the results were compared to FDS. For the empty tunnel and low air flow, the results were comparable. For obstacles in the tunnel and various air flow velocities, we found out it is not possible to use CFAST reliably for fires in the tunnels. Therefore, we used the one-dimensional model of the fire, similarly as in the document TP02/2011 [19], or in IDA RTV [6], with pre-determined curves of the fire power for each type of the vehicle. Shape of the curve for the fire power may be mathematically simplified either linearly, exponentially, or quadratically [20]. For simulation, we chose model curves of fire development according to real tests (Figure 5).

References [25, 26] give equation for calculation of temperature at the place of fire:

$$T_{\text{fire}} = \frac{Q}{v \rho A c_p} + T_0, \quad (9)$$

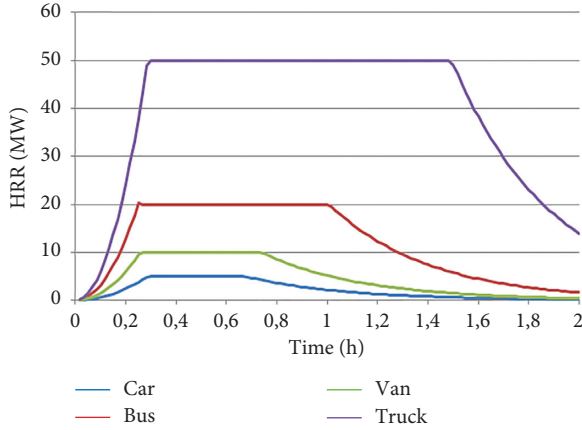


FIGURE 5: Model curves of the heat power of the fire.

where

- (1)  $Q$  is the fire power (W)
- (2)  $v$  is the velocity of air flow (m/s)
- (3)  $\rho$  is the air density ( $\text{kg/m}^3$ )
- (4)  $A$  is the area of cross section of the tunnel ( $\text{m}^2$ )
- (5)  $T_0$  is the outside temperature (K)
- (6)  $c_p$  is the specific heat capacity of air ( $\text{kJ}/(\text{kgK})$ )

Since we have the one-dimensional model, temperature is considered as an average temperature of the cross section at the place of fire. According to [25], comparison with the three-dimensional computational fluid dynamics (CFD) simulation in situations without backflow of the smoke gives a good coincidence of temperatures (error ca 1%). In the case of backflow of the smoke, an error occurs. Burning efficiency is not 100% so the power in equation must be reduced. We chose the value 90%. Further, we applied only a part of the reduced power of the fire, approximately 70%, in accordance with the references; the residual power is radiated to the wall of the tunnel. For its temperature, we can use the following equation [22]:

$$Q_{\text{wall}} = \varepsilon \delta (T_{\text{fire}}^4 - T_{\text{wall}}^4) \pi D L_{\text{FIRE}} + \alpha (T_{\text{fire}}^4 - T_{\text{wall}}^4) \pi D L_{\text{FIRE}}, \quad (10)$$

where

- (1)  $\varepsilon$  is the emissivity (-)
- (2)  $\delta$  is the Stefan-Boltzmann constant ( $\text{W}/(\text{m}^2\text{K}^4)$ )
- (3)  $\alpha$  is the coefficient of the heat transfer ( $\text{W}/(\text{m}^2\text{K})$ )
- (4)  $T_{\text{wall}}$  is the temperature of the wall (K)
- (5)  $T_{\text{fire}}$  is the air temperature (K)
- (6)  $L_{\text{FIRE}}$  is the length of the tunnel with fire (m)
- (7)  $D$  is the hydraulic diameter of the tunnel (m)

The given equation considers radiation to tunnel walls one-dimensionally; there is difference between the ceiling and the pavement.

Generally, the fire may be detected by multiple ways. For our simulations, there were more important autonomous

systems: smoke detection and linear detector FibroLaser [27]. For simulations, we used variable detection time.

**3.5. Smoke Propagation Model.** Smoke propagation depends on velocity of air flow in the tunnel, size of the fire, cross section of the tunnel, and the tunnel gradient. Smoke whose temperature is higher than temperature of air in the tunnel is propagated below the ceiling and depending on velocity of air flow it propagates one way or both ways. Figure 6 shows possibilities of smoke propagation in the tunnel.

In Figure 6(a), velocity of air flow is low, and smoke stratifies evenly. Fire ventilation in the tunnel for both-way operation should follow this case since there are persons along both sides of place of fire. In Figure 6(b), velocity of air flow is lower than critical velocity, and smoke destratification occurs, backflow propagation of the smoke. In Figure 6(c), velocity of air flow is higher than critical velocity, and smoke destratification does not occur. For one-way traffic, knowledge of critical velocity for fires of various vehicle types is key knowledge for safety of persons in the tunnel. Comparison of various ways of how to calculate critical velocity in dependency on fire power is shown in Figure 7. For the simulation, we chose an analytical calculation [27].

The critical expression of critical speed was chosen for its optimality with respect to all commonly used approaches to the calculation of critical speed. The comparison was made based on the authors' analysis method [29] and calculation using software IDK RTV, TP12/2011.

According to the technical conditions of ventilation of road tunnels TP12/2011, this speed for longitudinal ventilation in the direct of traffic in one-way traffic should be greater than the so-called critical speed at which smoke spreads back. If people are only in one direction from the fireplace, fire ventilation has to be controlled, so that flow speed in higher than or equal to the critical speed.

Calculation of critical speed according to TP12/2011 is as follows:

$$v_{\text{crit}} = C_0 C_3 \sqrt{C_1 C_4} \frac{\sqrt{1 + (1 - (C_2/C_1)) C_4 (B^2/gH)}}{1 + C_4 (B^2/gH)} B, \quad (11)$$

where input values are

$Q = 5.106 \text{ W}$  for a car fire, the amount of the heat released,

$g = 9,81 \text{ m.s}^{-2}$  gravitational acceleration,

$c_p = 1039 \text{ J}/(\text{kg.K})$  heat capacity of the clean air stream,

$H = 6,995 \text{ m}$  clearance height of tunnel,

$W = 9,5 \text{ m}$  clearance width of tunnel,

$A = 57,26 \text{ m}^2$  area of clearance cross section tunnel,

$s = 1\%$  gradient of tunnel,

$a = 1,134 \text{ kg/m}^3$  flow density of clean air,

$T_a = 288,15 \text{ K}$  clean air flow temperature.

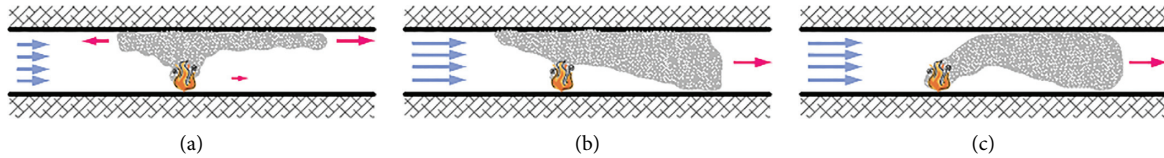


FIGURE 6: Smoke propagation depending on velocity of air flow [28].

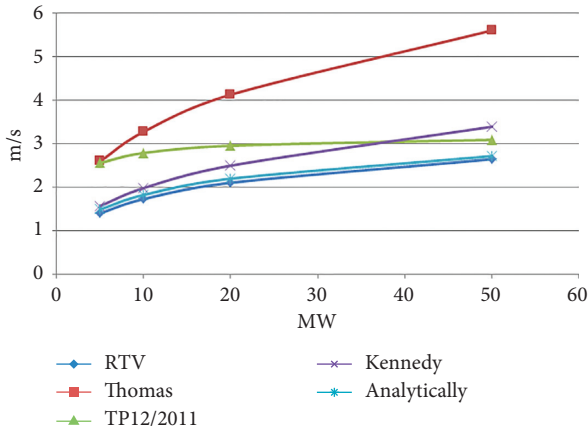


FIGURE 7: Comparison of various ways of critical velocity calculation.

The constant values of highway double-tube tunnel are  $C0 = 0, 9$ ,  $C1 = 0, 91935$ ,  $C2 = 0, 42233$ ,  $C3 = 0, 61299$ ,  $C4 = 7, 51768$ .

For different scenarios of vehicle fire, only coefficient  $B$  is changed:

$$B = \sqrt[3]{\frac{QgH}{c_p T_a \rho_a A}} \quad (12)$$

- 5 MW :  $B = 2,6036$ ,  $v_{crit} = 2,565$  m/s,
- 10 MW :  $B = 3,2803$ ,  $v_{crit} = 2,794$  m/s,
- 20 MW :  $B = 4,1329$ ,  $v_{crit} = 2,961$  m/s,
- 50 MW :  $B = 5,6093$ ,  $v_{crit} = 3,097$  m/s.

**3.6. Fire Ventilation Algorithm.** We analysed the control algorithm of fire ventilation for traffic volume 1600 (veh/h) and for the values 5 MW and 50 MW of firepower. For comparison, we chose the following ways to control ventilation: switching of all the fans off, switching of three fans on (half of all except for the fire zone), switching of six fans on (all except for the fire zone), and regulation to the required value within the interval from 3 to 3.5  $ms^{-1}$  with the steps 30 s and 60 s. The control system activated the chosen way of ventilation control in the 5<sup>th</sup> minute from stopping the traffic. The result of comparison for 5 MW is shown in Figure 8, and for 50 MW in Figure 9. In the 20<sup>th</sup> minute, we suddenly chose velocity of the wind 4 (m/s) in the opposite direction to assess decrease in the flow value. We can see that for deactivated ventilation velocity of the flow decreases under the value of the critical velocity at the time 800 s, i.e., approximately 8 minutes after traffic had been stopped. For

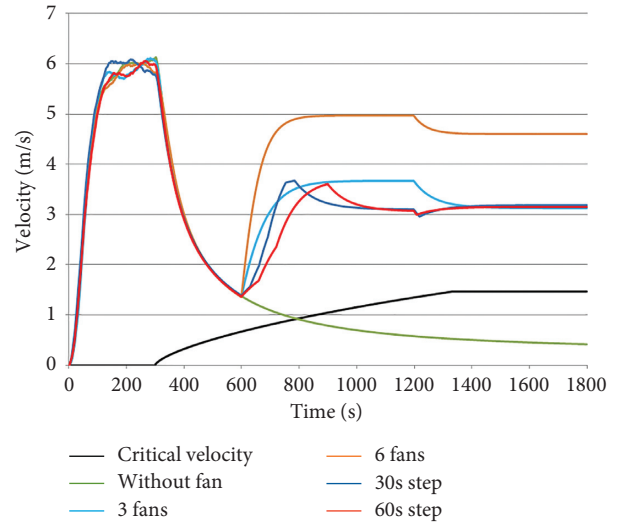


FIGURE 8: Comparison of algorithms of ventilation control for 5 MW fire.

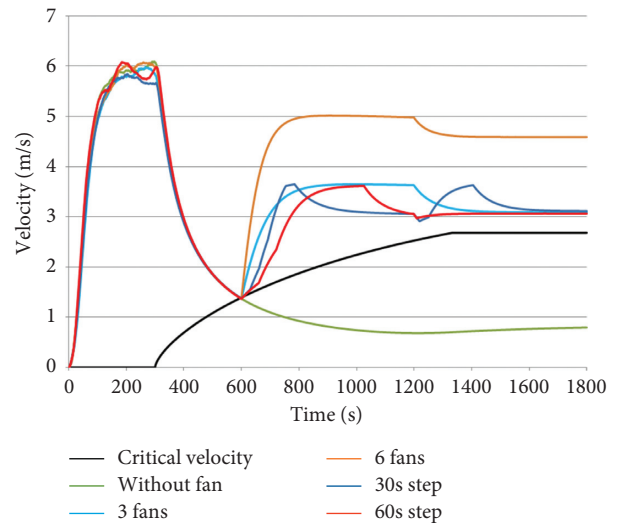


FIGURE 9: Comparison of algorithms of ventilation control for 50 MW fire.

5 MW fire and the fixed number of switched-on fans, the value of velocity of the flow did not decrease below the value 3 (m/s), even for 3 fans. It means that condition of 100 % redundancy of fans was fulfilled. When regulating to the required value of the air velocity, we can see that the step 30 s has a steeper rise to the required value, but a higher overshoot as well. The error caused by the wind was in both cases immediately compensated by increase in fire; fire reached its maximum in time of the constant value of critical velocity.

For 50 MW, we can see that reaction of the control system 5 minutes after stopping traffic is already at the critical value of velocity for the given fire. Similarly, as in the previous comparison, only three fans were sufficient to keep the value of air flow 3 (m/s), so again the requirement of 100% redundancy of fans was fulfilled. Higher velocity of air flow guarantees lower temperature of air in front of the fire place, ensures delivery of fresh air, and keeps smoke in direction from evacuating persons. The maximum value of velocity of air flow in the opposite direction should not be problematic for them.

**3.7. Evacuation Model.** As we can see from Figure 10, velocity of persons moving within the smoky space decreased even for the value of opacity 0.4 – (1/m). That value also changed based on position of persons in the tunnel, the tunnel did not get smoky immediately along the whole length, and the evacuating model should consider it.

The study of the smoke/speed correlation is currently based on two main datasets:

Set of experiments from Jin [1976]

Set of experiments from Frantzich and Nilsson [2003]

The first dataset (from Jin) collected data and they were used for providing correlation between the extinction coefficient and walking speeds, visibility levels, and cognitive abilities when exposed to smoke.

Jin used two types of different smoke. First was irritant smoke, which was produced by burning wood cribs. Second was non-irritant smoke, which was produced by burning kerosene. This experiment was performed in 20-meter long corridor that was filled with smoke corresponding to an early stage of fire. The experiment involved 17 women and 14 men, ranging from 20 to 51 years in age.

The second dataset (from Frantzich and Nilsson) is from more recent studies. This experiment was performed in tunnel for studying the influence of different visibility conditions on individual walking speeds.

Frantzich and Nilsson used artificial smoke and, for simulation irritation, acetic acid was used. This experiment was performed in 37-meter long tunnel tube. The experiment involved 46 people.

Cellular automaton (CA) model of traffic was extended for a number of persons inside vehicles; therefore, the evacuation model accepts an initial distribution of persons in the tunnel. Interconnection of the CA model of traffic and the evacuation model is shown in Figure 11.

To estimate speed of walking in the evacuation model, the following fuzzy inference system (FIS) was designed:

Density of persons (at the evacuation path): low (<1.5(person/m<sup>2</sup>), middle, and high (>4(person/m<sup>2</sup>))

Smokiness: low (<(2/m)), middle, and high (>(6/m))

Illumination (the level of operational lighting): low (<25%), middle, and high (>70%)

In the first step, all membership functions were chosen as trapezoidal and linguistic variables were deduced expertly. It

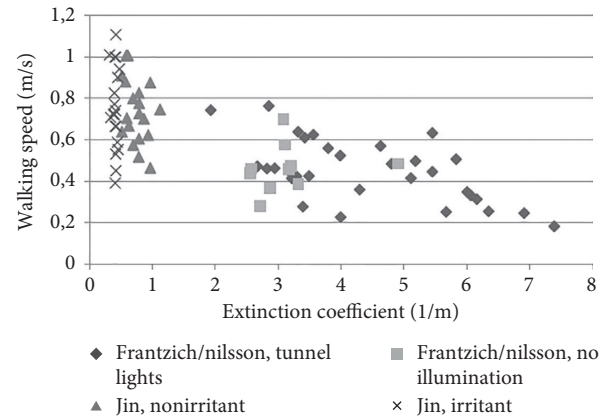


FIGURE 10: Walking speed of humans in smoky area, for switched-on and switched-off illumination [30].

turned out it was possible to reach lower deviation from experimental data when tuning the shape of membership function by genetic algorithms. Comparison of various approaches is documented in [31, 32].

To compare the evacuation model we decided to use data from [30] where detailed comparison of multiple evacuation tools is available. We repeated selected experiments with our evacuation model; comparison of input data for experiments is given in Table 1.

For all the scenarios, one-way traffic was applied, stopping at the emergency exit without switched-on ventilation. The scenarios A1.1, A1.2, and A2.1-A2.3 were analysed in [30]. The first two simulated a standard course of evacuation with its immediate initiation. Then, various walking speeds were tested. The average evacuation times for individual scenarios are given in Table 2 together with standard deviations (in parentheses).

#### 4. Risk Analysis in TuSim

The TuSim extended for mathematical-physical models is a model suitable for simulation experiments with technological equipment based on scenario analysis. To evaluate scenarios, it is appropriate to compare ASET (Available Safe Egress Time) and RSET (Required Safe Egress Time), or mortality rates for individual scenarios. Meaning of times RSET and ASET is apparent from Figure 12.

Figure 13 shows a clearer time-spatial way of visualization of times RSET/ASET [35], where there is no problem to assess the situation at the particular place in the tunnel. On the left side of the picture, there is velocity of air flow indicated; on the right side of the picture, there is smoke propagation shown and the red lines represent escape paths to individual exits.

The way used to make simulation in TuSim is depicted in Figure 14. Setting of the simulation parameters is in the top left corner of the picture. In the top right part of the picture, there is the course of simulation for unstopped traffic and in the bottom right part for stopped traffic and evacuated persons.



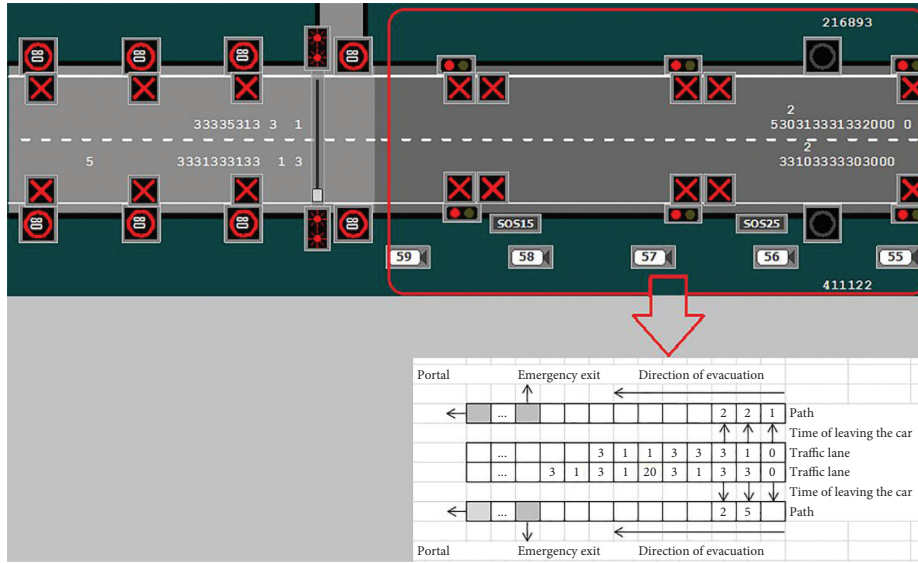


FIGURE 11: Interconnection of the evacuation with the CA model of traffic.

TABLE 1: Comparison of the evacuation models.

	Ronchi	TuSim
Tunnel length	670 m	675 m
Distance to emergency exit	390 m	390 m
Width of the path	2.5 m, 0.75 m	1.5 m, 1.5 m
Length of the vehicle	Car: 4.5 m + gap 1 m Truck: 10 m	7, 5 m with gaps
Number of persons in the vehicle	Cars: 2.5–5 trucks: 1-2	Cars: 3-6 trucks: 1-2
Number of persons in the tunnel	A1.1, A2.2: 312 persons, A2.1, A2.1, A2.3: 624 persons	Variable ~300 variable ~600

TABLE 2: Results of comparison of evacuation models.

Scenario	SFPE	FDS + EVACS	STEPS	Pathfinder	TuSim
A1.1	—	403	402	400	399 (16, 7)
A1.2	—	406	402	400	426 (11, 8)
A2.1	578	577 (18, 1)	583 (15, 4)	584 (12, 5)	583 (16, 6)
A2.2	508	545 (22, 6)	529 (19, 5)	535 (23, 1)	548 (23, 4)
A2.3	526	571 (6, 9)	535 (7, 9)	675 (17, 8)	562 (13, 9)

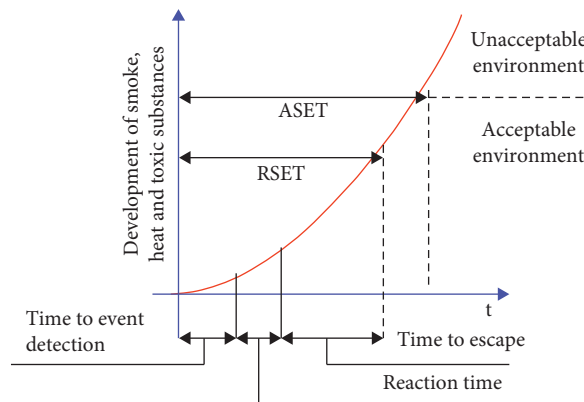


FIGURE 12: Meaning of times RSET and ASET [33].

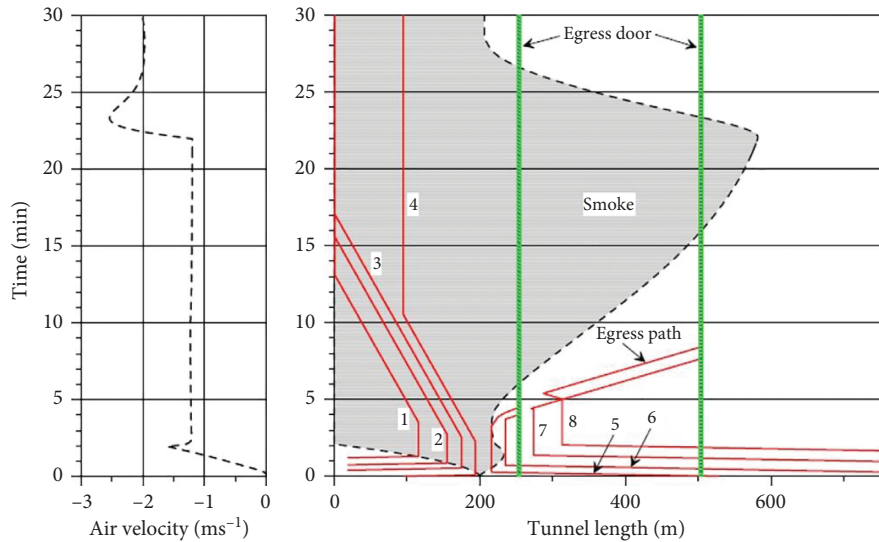


FIGURE 13: Graphical output of simulation of smoke propagation and escape paths [34].

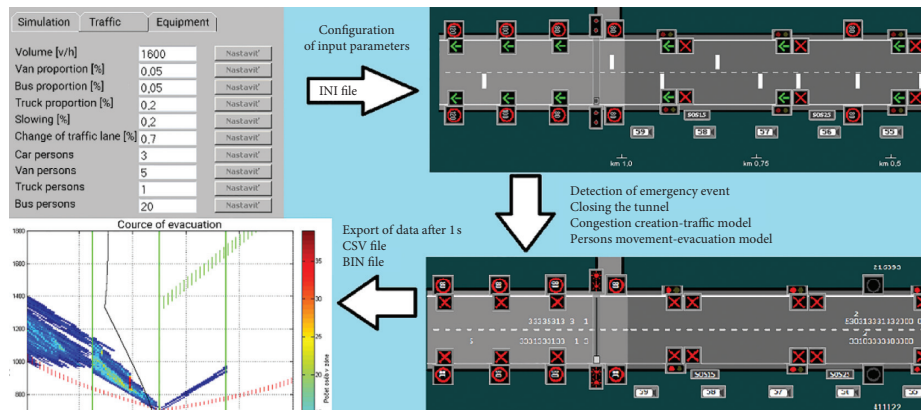


FIGURE 14: TuSim, simulation experiment.

## 5. Evaluation

We set the same conditions for scenarios:

Stopping of one-way traffic with the volume 1600 (veh/h) in the 300th minute of simulation

Response of the control system in the 600th minute of simulation

We were interested in the best case (switching-on of three pairs) and the worst case (switching-on of no fan).

To simulate the humans' decisions to evacuate, we used the rule of temperature increased to 45°C or smoke present at the place of human appearance. If none of the rules applied, we started evacuation in the 900th minute with time penalization according to distance from the place of fire. For each scenario, we showed time-spatial way of time visualization RSET/ASET, where red hatching indicates the value of air temperature 50 – 55°C.

Figure 15 shows that for fire of the truck velocity of air flow shortly decreased below the estimated value of critical velocity and backflow of smoke may occur for a short period

of time. Increased temperature will cause earlier initiation of evacuation; temperature 50°C will reach emergency exit behind the fire place approximately in the 960th minute. If persons started evacuation in a wrong direction, in addition to smoke they will be endangered by heat as well.

Figure 16 shows the course of truck fire with switched-off ventilation where smoke backflow does not reach the emergency exit in front of the place of fire due to increased velocity of air flow to 1 (m/s). The persons complete evacuation by 1404 s. Temperature 50°C will reach the emergency exit behind the place of fire approximately by the 13th minute, emergency exit in front of the place of fire approximately by the 14th minute, and the whole evacuation of persons will run in environment with higher temperature. Higher temperature need not immediately cause inability of persons to evacuate, and smoke backflow below the ceiling of the tunnel need not immediately endanger persons. The smoke of the fire will start to mix with bottom layers of the air, even after partial cooling of the gas, and this effect can be very difficult considered in one-dimensional simulation models.

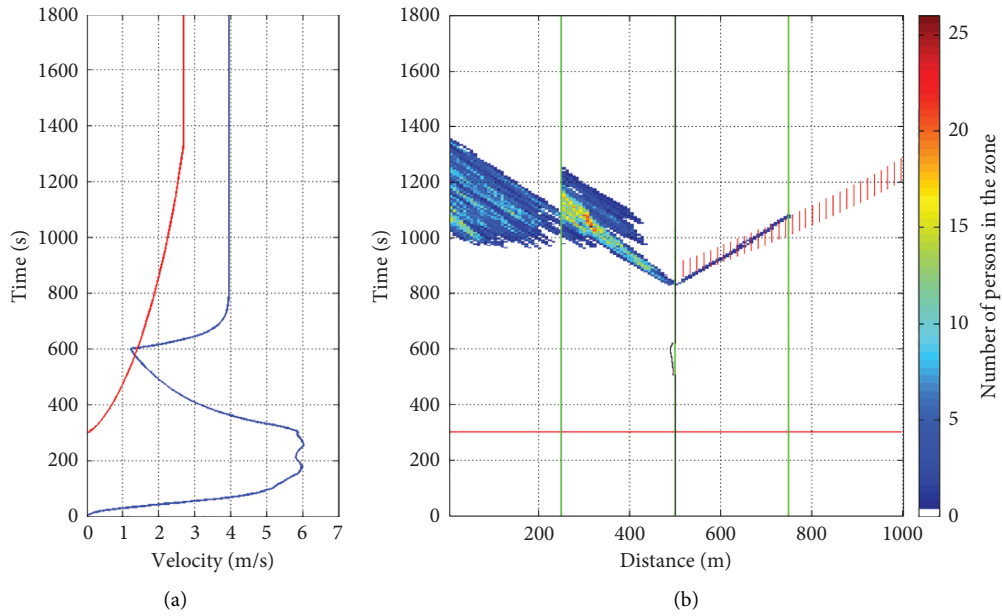


FIGURE 15: Course of evacuation for the truck fire with switched-on ventilation [36]. (a) Velocity of air flow. (b) Course of evaluation.

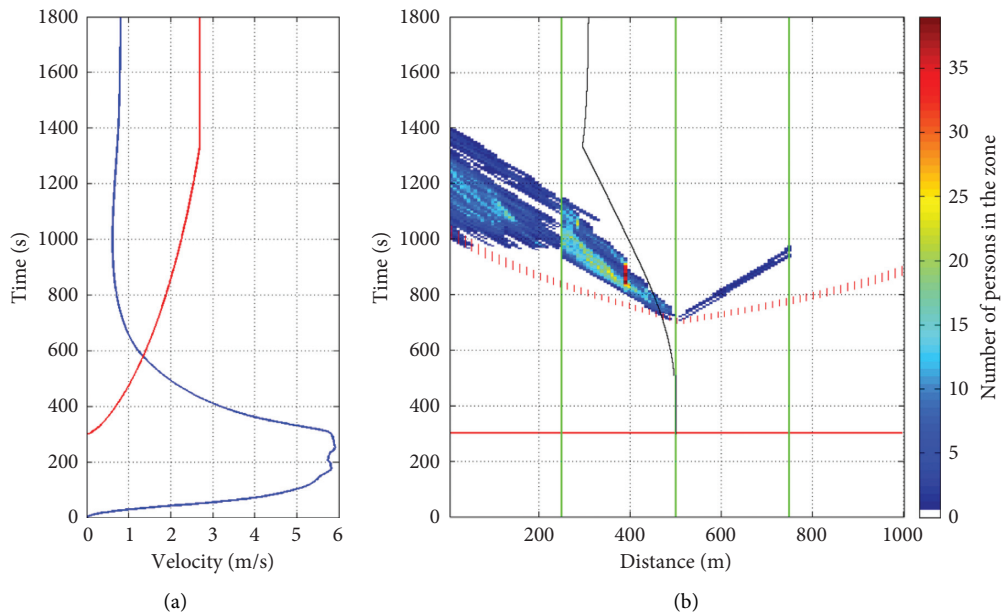


FIGURE 16: Course of evacuation for the truck fire with switched-off ventilation. (a) Velocity of air flow. (b) Course of evaluation.

Persson [34] utilized the one-dimensional model of the fire and used a fractional effective dose (FED) and fractional incapacitating dose (FID) for mortality calculation. For scenarios of vehicle fire, they got zero mortality, fatalities were caused only by the fire of dangerous goods, or fire with near to immediate increase to maximum power (explosive conflagration). For working ventilation, those findings are following our conclusions.

Three-dimensional simulations in the Horelica tunnel [37] revealed that temperature in the upper air mass in the height 1.8 m is not dangerous for humans in none of the analysed scenarios. The results are not valid for

immediate surroundings of the fire, i.e., up to 10 m in front of the fire and behind it. In the direction of airflow, the temperature exceeded the value 50°C along the whole length of the tunnel tube for the fires 20 MW and 50 MW which corresponds to our findings for the lower velocities of airflow. For 50 MW fire, radiation above the level 2.5 kW/m<sup>2</sup> mostly endangered persons being the max. 25 m in the direction of airflow which corresponds to our calculated value of the distance 25.69 m for the same radiation and fire.

We can see that for the tunnel 1 km long we can keep the airflow in the direction of traffic only if fire detection and the

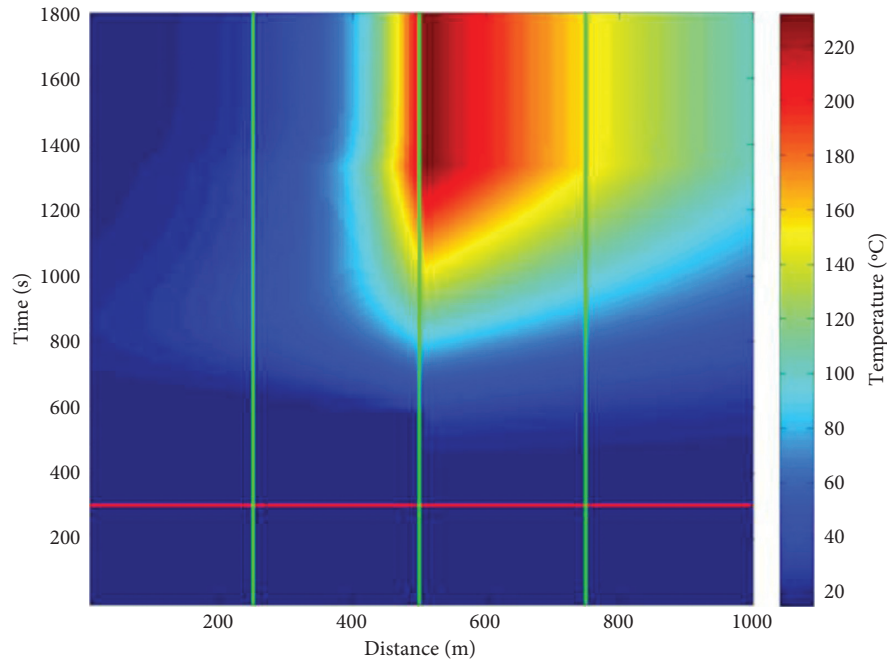


FIGURE 17: Development of temperature over space and time.

following start of the ventilation will occur within 5 minutes from the traffic stop. In the case of the correct function of fire detection and ventilation systems, without irrational behavior of the persons (evacuation in a wrong direction), without staying in vehicles, there will be no fatalities for one-way traffic.

In the case of two-way traffic, a part of persons will evacuate in a smoke environment with low visibility. Switching the ventilation off may be problematic in short tunnels due to a change in the airflow. Possible regulation to the given value of airflow, e.g., the particular values 0 or 1 m/s according to technical conditions, may be reachable with difficulties without the possibility to change the ventilation airflow (frequency inverters, fan blades angle of attack control, etc.).

## 6. Detection of Fire by the Vehicle

In the previous sections, we have proposed a method to simulate the physical conditions (opacity, temperature, air speed, carbon oxide concentration, etc.) inside the road tunnel in case of fire. As one could see in Figure 16, if the tunnel ventilation is not working, evacuating persons will be endangered by high temperature and smoke. Figure 17 shows temperature development over space and time inside the tunnel. First detectable rising of the temperature occurs at 600 s, but people will start to evacuate at 700 s. During those 100 s, the temperature will rise by approx. 20°C. The fire can be therefore detected in advance comparing the normal temperature inside the tunnel (computed by the TuSim without the event of fire) and the real measured temperature. If the temperature is above the maximal normal temperature and the vehicle is steady, there is a high possibility of the fire inside the tunnel and the autonomous

vehicle has to issue an alert to its passengers prompting them to the nearest egress exit. Similar approach can utilize measurement of COx concentration indicating the presence of the smoke.

The alarm inside the vehicle should be issued when any of these conditions is met:

Vehicle is steady, and the temperature is above maximal normal temperature at given distance inside the tunnel

Vehicle is steady, and the concentration of COx is above the maximal normal level at given distance inside the tunnel

The maximal normal values for temperature and exhaust gasses concentration will be provided by TuSim for given parameters of the traffic and the tunnel. These values depend on the distance. The distance of the vehicle from the portal of the tunnel can be estimated by odometers inside the vehicle combined with other sensors used in autonomy navigation.

## 7. Conclusion

The article proposes a complex simulation method in order to predict the development of the physical properties (e.g., temperature, opacity) in case of fire inside the road tunnel. When evaluating an effect of the technological equipment in case of fire in the road tunnel, we must realize a detailed time-spatial analysis of the given event. The methods based on statistics are not able to consider effect of technologies when an event occurs. The correct functionality of detection and reaction of the tunnel control system is usually assumed. Further, the results from the statistics cannot be scaled linearly with the parameters of the tunnel. The only option is to perform a simulation experiment. An

advantageous option for simulation experiments is the use of PLC, as real control systems are built on the same platform. As a starting point of our work, we have used our TuSim tunnel simulator.

Once the possible scenarios (fire with different power) are computed, the predicted normal and critical behaviour of the tunnel along with the location of the emergency exits may be presented to the intelligent vehicles. The vehicles may detect the fire early considering changes in temperature and opacity. The proposed method is independent of the external systems in case of emergency (wireless communication inside the tunnel may fail in case of fire). Therefore, the passengers will be alerted even when the communication link with the tunnel is lost.

## Data Availability

The data supporting the conclusions of this study are from the following: Miklóšik, I., Pokročilé metódy kvantifikácie bezpečnosti cestných tunelov. PhD. work, Faculty of Electrical Engineering and Information Technology, University of Žilina, 2016, [http://kris.uniza.sk/images/dokumenty/EU\\_CEx\\_IDS.pdf](http://kris.uniza.sk/images/dokumenty/EU_CEx_IDS.pdf) <http://kris.uniza.sk/veda-vyskum-prax/grant-ulohy>.

## Conflicts of Interest

The authors declare that there are no conflicts of interest regarding the publication of this paper.

## Acknowledgments

This work was supported by Slovak Research and Development Agency under APVV-17-0014.

## References

- [1] B. Luin, S. Petelin, and P. Vidmar, "Interactive model OF a road tunnel during," in *Proceedings of the 14th International Conference on Transport Science - ICTS 2011*, p. 10, Portorož, Slovenia, 2011.
- [2] Federal Highway Administration of Transport. Federal Highway Administration of Transport. <https://www.fhwa.dot.gov/>.
- [3] EQUA Simulation, "IDA road tunnel ventilation 3.0," 2017, [http://www.ilg-engineering.ch/Tunnelsicherheit/IDA\\_Tunnel\\_brochure.pdf](http://www.ilg-engineering.ch/Tunnelsicherheit/IDA_Tunnel_brochure.pdf).
- [4] Časopis Českého Tunelářského Komitétu a Slovenskej Tunelárskej Asociácie ITA/AITES. [http://www.ita-aites.cz/files/tunel/komplet/tunel\\_4\\_07.pdf](http://www.ita-aites.cz/files/tunel/komplet/tunel_4_07.pdf).
- [5] I. R. Riess, P. Altenburger, and P. Sahlin, "On the design and control of complex tunnel ventilation," in *Proceedings of the 12th Int. Symp. Aerodynamics and Ventilation of Vehicle Tunnels*, p. 11, Portoroz. Portoroz, 2006.
- [6] GE Fanuc Automation, "CIMPLICITY HMI plant edition," 2017, <http://platforma.astor.com.pl/files/getfile/id/4664>.
- [7] GE Fanuc Automation, "CIMPLICITY HMI plant edition - CimEdit operation manual," 2017, <http://platforma.astor.com.pl/files/getfile/id/4675>.
- [8] LIBNODEAVE, "Exchange data with Siemens PLCs," 2017, <http://libnodave.sourceforge.net/>.
- [9] Mathworks, "Matlab help," 2017, <http://www.mathworks.com/help/matlab/index.html>.
- [10] I. Miklóšik, J. Spalek, M. Hruboš, and P. Příbyl, "Cellular automaton traffic flow model with vehicle type and number of persons," in *Archives of Transport System Telematics* sp. 5, PSTT, Wroław, Poland, 2015.
- [11] I. Miklóšik and J. Spalek, "Extension of the tunnel simulator with the traffic flow model," in *Telematics - Support for Transport*, J. Mikulski, Ed., Springer, Ustroń, Poland, pp. 156–165, 2014.
- [12] H. J. Fernando, *Handbook of Environmental Fluid Dynamics, Volume Two: Systems, Pollution, Modeling, and Measurements*, CRC Press, vol. 12, p. 587, Boca Raton, FL, USA, 2012.
- [13] D. Wei and W. Ge, "Research on one bio-inspired jumping locomotion robot for search and rescue," *International Journal of Advanced Robotic Systems*, vol. 11, no. 10, p. 168, 2014.
- [14] L. Kurka, L. Ferkl, O. Sládek, and J. Porízek, "Simulation of traffic, ventilation and exhaust in a complex road tunnel," in *Proceedings of the IFAC Volumes (IFAC-PapersOnline); 2005*, pp. 60–65, IFAC, Prague, Czech Republic, July 2005.
- [15] Comité technique AIPCR, "Exploitation des tunnels routiers/ PIARC Technical Committee C.4 Road Tunnel Operation. Road tunnels: vehicle emissions and air demand for ventilation," *Environment/Road Tunnel Operations*, vol. 87, 2012.
- [16] P. Lunardi, G. Cassani, M. Gatti, G. Lodigiani, M. Frankovský, and M. Fulvio, "The ADECO-RS approach and the full-face excavation," *Tunely a podzemné stavby*, vol. 11, p. 12, 2015.
- [17] Y. Z. Li, C. G. Fan, H. Ingason, A. Lönnemark, and J. Ji, "Effect of cross section and ventilation on heat release rates in tunnel fires," *Tunnelling and Underground Space Technology*, vol. 51, pp. 414–423, 2016.
- [18] M. Pavelka and P. Příbyl, *Simulace Pohybu Vzduchu a Škodlivin V Tunelu-Matematický Model*, ČVUT v Praze Fakulta Dopravní, Konviktská, Czechia, 2006.
- [19] M. dopravy and S. R. výstavby a regionálneho rozvoja, "Analýza rizík pre slovenské cestné tunely," 2017, [http://www.ssc.sk/files/documents/technicke-predpisy/tp2011/tp\\_02\\_2011.pdf](http://www.ssc.sk/files/documents/technicke-predpisy/tp2011/tp_02_2011.pdf).
- [20] National Cooperative Highway Research Program (NCHRP), *Synthesis 415: Design Fires in Road Tunnels*, National Cooperative Highway Research Program (NCHRP), Washington, DC, 2011.
- [21] D. Gola, *Simulace Aerodynamického Chování*, <https://dspace.cvut.cz/bitstream/handle/10467/61855/F3-BP-2015-Gola-Daniel-priloha-bakalarska-prace.pdf>, p. 59, České vysoké učení technické v Praze, Prague, Czech Republic, 2015, .
- [22] I. Riess and M. Bettelini, "The prediction of smoke propagation due to tunnel fires," in *Proceedings of the ITC Conference Tunnel Fires and Escape from Tunnels*, p. 18, Lyon, France, 1999.
- [23] NIST - National Institute of Standards and Technology, "CFAST, Fire Growth and Smoke Transport Modeling," 2017, <https://www.nist.gov/el/fire-research-division-73300/product-services/consolidated-fire-and-smoke-transport-model-cfast>.
- [24] S. Tavelli, R. Rota, and M. Derudi, "A critical comparison between CFD and zone models for the consequence analysis of fires in congested environments," *Chemical Engineering Transactions*, vol. 36, p. 6, 2014.
- [25] Bundesministerium für Verkehr, Innovation und Technologie . Betrachtung der Wärmefreisetzung im Brandfall. [https://www.bmvit.gv.at/service/publikationen/verkehr/strasse/downloads/tunnel\\_laengslueftung.pdf](https://www.bmvit.gv.at/service/publikationen/verkehr/strasse/downloads/tunnel_laengslueftung.pdf).
- [26] I. Riess and M. Bettelini, "Smoke extraction in tunnels with considerable slope," in *Proceedings of the 4th International*

- Conference Safety in Road and Rail Tunnels*, pp. 503–512, Madrid, Spain, 2001.
- [27] I. Miklóšik, P. Kello, and J. Spalek, “Fiber laser fire detection in the tunnel simulator,” in *Proceedings of the 2016 ELEKTRO*, pp. 429–434, IEEE, Strbske Pleso, Slovakia, 2016.
- [28] S. A. T. RA. Kvantitativní Analýza Přepravy Nebezpečných Nákladů Silničním Tunelem Sitina V Bratislavě. <http://www.ita-aites.cz/files/tunel/2007/3/tunel-0703-5.pdf>.
- [29] M. Banjac, “Numerical study of smoke flow control in tunnel fires using ventilation systems,” *FME Transactions*, vol. 36, p. 2008, 2008.
- [30] E. Ronchi, “Evacuation modelling in road tunnel fires,” 2008, <http://lup.lub.lu.se/search/ws/files/5519346/4001478.pdf>.
- [31] M. Gregor, I. Miklóšik, and J. Spalek, “Automatic tuning of a fuzzy meta-model for evacuation speed estimation,” in *Proceedings of the 2016 Cybernetics & Informatics (K&I)*, pp. 1–6, Levoca, Slovakia, 2016.
- [32] P. Matis and J. Spalek, “ATP journal plus 2/2013 - fuzzy model doby reakcie osôb v cestnom tuneli pri vzniku mimoriadnej udalosti,” 2017, [http://www.atpjournalsk/buxus/docs/casopisy\\_cele/ATP\\_PLUS\\_2\\_2013\\_zmensene.pdf](http://www.atpjournalsk/buxus/docs/casopisy_cele/ATP_PLUS_2_2013_zmensene.pdf).
- [33] I. Riess and R. Brandt, “A one-dimensional egress model for risk analysis,” in *Proceedings of the Symposium Tunnel Safety and Ventilation*, vol. 5, pp. 165–172, Graz, Austria, 2010.
- [34] A. Osvald, V. Mózer, and J. Svetlík, *Požiarna Bezpečnosť Cestných Tunelov*, p. 140, EDIS, Žilina, Slovakia, 2014.
- [35] M. Persson, “Quantitative risk analysis procedure for the fire evacuation of a road tunnel,” 2017, <https://lup.lub.lu.se/luur/download?func=downloadFile&recordOID=1688790&fileOID=1765306>.
- [36] P. Kello, I. Miklóšik, J. Spalek, and T. Tichý, *The Comparison of Selected Fire Scenarios with TuSim*, ELEKTRO, Mikulov. Czech Republic, pp. 1–4, 2018.
- [37] J. Hrbcek and V. Šimák, “Implementation of multi-dimensional model predictive control for critical process with stochastic behavior,” *Advanced Model Predictive Control*, pp. 109–124, 2011.